Anisotropic diffraction from photorefractive gratings and Pockels tensor of $Sn_2P_2S_6$

Alexandr Volkov,[1] **Alexandr Shumelyuk,**[1] **Serguey Odoulov,**[1]
Dean R. Evans[2] **and Gary Cook,**[2,3]

[1]*Institute of Physics, National Academy of Sciences, 46, Science Avenue, 03650 Kiev, Ukraine*
[2] *Air Force Research Laboratory, Materials and Manufacturing Directorate, Wright-Patterson Air Force Base, Ohio 45433, USA*
[3] *Universal Technology Corporation, 1270 N. Fairfield Road, Dayton, Ohio, 45432, USA*
odoulov@iop.kiev.ua

http://www.iop.kiev.ua/~prc/

Abstract: The first observation of anisotropic diffraction and anisotropic self diffraction in low symmetry photorefractive crystal $Sn_2P_2S_6$ is reported. From comparison of the diffraction efficiency of isotropic and anisotropic diffraction the ratios of the Pockels tensor components are deduced, including some nondiagonal components that have never been evaluated until now. The particular orientation of the optical indicatrix in $Sn_2P_2S_6$ (roughly at 45° to *z*- and *x*-axes at ambient temperature) has a paradoxical consequence: The efficiency of anisotropic diffraction depends solely on diagonal components of the Pockels tensor, while the efficiency of the isotropic diffraction is considerably affected by nondiagonal components. With already known results and data presented in this article we can state that all 10 nonvanishing Pockels tensor components of the *m*-symmetry class crystal like $Sn_2P_2S_6$ do manifest themselves in various types of nonlinear wave mixing.

OCIS codes: (050.7330) Volume gratings; (160.2100) Electro-optical materials; (190.4380) Nonlinear optics, four-wave mixing; (190.5330) Photorefractive optics.

References and links

1. A. Grabar, M. Jazbinšek, A. Shumelyuk, Yu. M. Vysochanskii, G. Montemezzani, and P. Günter, "Photorefractive effects in $Sn_2P_2S_6$," in *Photorefractive materials and their applications 2*, P. Günter, and J.-P. Huignard, eds. (Springer-Verlag, 2007), pp. 327–362.
2. C. D. Carpentier, R. Nitsche, "Ferroelectricity in $Sn_2P_2S_6$," Mat. Res. Bull. Pergamon Press, Inc. **9,** 1097–1100 (1974); C. D. Carpentier and R. Nitsche, "Vapour growth and crystal data of the tio(seleno)-hypodiphosphates $Sn_2P_2S_6$, $Sn_2P_2Se_6$, $Pb_2P_2S_6$, $Pb_2P_2Se_6$, and their mixed crystals," Mater. Res. Bull. **9,** 401–410 (1974).
3. A. Shumelyuk, S. Odoulov, O. Oleynik, G. Brost, and A. Grabar, "Spectral sensitivity of nominally undoped photorefractive $Sn_2P_2S_6$," Appl. Phys. B **88,** 79–82 (2007).
4. Roger Mosimann, M. Jazbinšek, G. Montemezzani, A. Grabar, and P. Günter, "High speed photorefraction at telecommunication wavelength 1.55 μm in $Sn_2P_2S_6$," Opt. Lett. **32,** 3230–3232 (2007).
5. A. A. Grabar, R. I. Muzhikash, A. D. Kostyuk, and Yu. M. Vysochanskiy, "Investigation of the switching process in the domain structure of ferroelectric $Sn_2P_2S_6$ by the dynamic holographic method," Sov. Phys. Solid State **33,** 1314–1316 (1991).
6. S. G. Odoulov, A. M. Shumelyuk, U. Hellwig, R. A. Rupp, A. A. Grabar, and I. M. Stoyka, "Photorefraction in tin hypothiodiphosphate in the near infrared," J. Opt. Soc. Am. B **13,** 2352–2360 (1996).

#100420 - $15.00 USD Received 21 Aug 2008; revised 15 Sep 2008; accepted 15 Sep 2008; published 8 Oct 2008

7. D. Haertle, G. Caimi, A. Haldi, G. Montemezzani, P. Günter, A. A. Grabar, I. M. Stoika, and Yu. M. Vysochanskii, "Electro-optical properties of $Sn_2P_2S_6$," Opt. Commun. **215,** 333–343 (2003).
8. B. I. Sturman, S. G. Odoulov, and M. Yu. Goul'kov, "Parametric four-wave processes in photorefractive crystals," Phys. Rep. **275,** 197–254 (1996).
9. M. P. Petrov, S. J. Stepanov, and A. V. Khomenko, *Photorefractive Crystals in Coherent Optical Systems* (Springer-Verlag, Berlin, 1991).
10. D. Haertle, A. Guarino, J. Hajfler, G. Montemezzani, and P. Günter, "Refractive indices of $Sn_2P_2S_6$ at visible and infrared wavelengths," Opt. Express **13,** 2047–2057 (2005), http://www.opticsinfobase.org/abstract.cfm?URI=oe-13-6-2047.
11. Considerable difference of an optical frame and a dielectric frame has been pointed out recently for the other monoclinic crystal used as a laser active medium, Nd:YCOB, in publication Yannick Petit, Benoît Boulanger, Patricia Segonds, Corinne Félix, Bertrand Ménaert, Jullien Zaccaro, and Gérald Aka, "Absorption and fluorescence anisotropies of monoclinic crystals: the case of Nd:YCOB," Opt. Express **16,** 7997–8002 (2008), http://www.opticsinfobase.org/abstract.cfm?URI=oe-16-11-7997.
12. Daniel Haertle, "Photorefractive and nonlinear properties of $Sn_2P_2S_6$," PhD Thesis, ETH No. 16107, Zürich 2005, p.33.
13. ANSI/IEEE, Std 176 - IEEE Standard on Piezoelectricity, p.242 (IEEE, Inc; 345 East 47th Street, New York, NY 10017, USA, 1987).
14. G. Dittmar and H. Schäfer, "Die Stuktur des Di-Zinn-Hexathiohypodiphoshatus $Sn_2P_2S_6$," Zeitschrift für Naturforschung, **29B,** (5-6), 312–317 (1974).
15. S. Odoulov, "Spatiallty oscillating photovoltaic current in iron-doped lithium iobate crystals," Sov. Phys.: JETP Letters, **35**, 10–13(1984); S. Odoulov, "Vectorial interactions in photovoltaic media," Ferroelectrics **91,** 213–225 (1989).
16. N. Kukhtarev, and S. Odoulov, "Wavefront inversion in anisotropic self-diffraction of laser beams," Sov. Techn. Phys. Lett. **6,** 503–504 (1980).
17. N. V. Kukhtarev, E. Krätzig, H. C. Külich, R. Rupp, and J. Albers, "Anisotropic self diffraction in $BaTiO_3$," Appl. Phys. B **35,** 17–21 (1984).
18. A. Shumelyuk, A. Volkov, A. Selinger, M. Imlau, and S. Odoulov, "Frequency-degenerate nonlinear light scattering in low-symmetry crystals," Opt. Lett. **353,** 151–153 (2008).
19. L. Solymar, D. Webb, and A. Grunnet-Jepsen, *The Physics and Applications of Photorefractive Materials*, (Clarendon, Oxford, 1996).
20. A. Shumelyuk, D. Barilov, S. Odoulov, and E. Krätzig, "Anisotropy of the dielectric permittivity of $Sn_2P_2S_6$ measured with light-induced grating techniques," Appl. Phys. B **76,** 417–421 (2003).

1. Introduction

Tin hypothiodiphosphate ($Sn_2P_2S_6$, SPS) is a promising photorefractive material [1] that belongs to symmetry group *m* [2]. It is sensitive from the red up to the optical communication wavelengths 1.3 μm [3] and 1.5 μm [4] and has a fast response (down to millisecond range in the visible) and a high gain factor (typically about 10 cm^{-1} but with some dopants up to 30 cm^{-1} in the visible) [1].

In spite of the fact that it was first synthesized in 1974 [2] and its photorefractive properties were discovered already more than decade ago [5,6] the dielectric and electrooptic properties of this crystal are still not fully characterized. In a recent publication [7] four of ten nonvanishing components of Pockels tensor were tabulated. They were extracted from the measurements of birefringence using the conventional technique with an external field applied to the sample. In this paper we describe some parametric wave mixing processes [8] that can be considered as optical manifestations of several previously unknown components of the Pockels tensor and we give the relative values normalized to the component r_{xxx} and r_{zzz}.

In particular, the first observation of anisotropic diffraction and self diffraction (diffraction with the change of polarization of the diffracted beam to orthogonal as compared to the polarization of the readout beam [9]) is reported for the samples cut along the crystallographic directions (*x*-cut, *y*-cut, and *z*-cut), with the appropriate orientation and polarization of the recording waves. With the known birefringence of SPS [10], the Bragg angles are calculated for all possible processes of anisotropic diffraction and particular types of diffraction are identified from comparison with the measured data. The effective electrooptic coefficients are then evaluated

#100420 - $15.00 USD Received 21 Aug 2008; revised 15 Sep 2008; accepted 15 Sep 2008; published 8 Oct 2008

for all studied geometries. The measured efficiency of these mixing processes and the diffraction efficiency of conventional isotropic diffraction (with identical polarization of incident and diffracted waves) enables the ratios of relevant Pockels coefficients involved in the grating readout to be found.

2. Definitions

For low symmetry crystals like SPS, different physical properties are defined in different Cartesian coordinates. The principal axes of the refraction index ellipsoid do not coincide, e.g., with the axes where the Pockels tensor is defined. The low frequency dielectric permittivity tensor in standard crystallographic coordinates contains nondiagonal components thus proving that dielectric frame is different from crystallographic frame [11]. This complicates the all-optical evaluation of the electrooptic coefficients compared with uniaxial photorefractive crystals that belong, for example, to 3*m* or 4*mm* symmetry classes like $LiNbO_3$, $LiTaO_3$, SBN or $BaTiO_3$. On the other hand, this complication brings new, sometimes quite unexpected effects, such as the independence of some kinds of anisotropic diffraction from the nondiagonal components of Pockels tensor.

In what follows we choose the Cartesian settings for SPS as proposed in [10,12]. In accordance to the IEEE standard on piezoelectric materials [13], the *z*-axis is defined parallel to the [001] crystallographic direction (axis *c*), while the *y*-axis is normal to the mirror plane and corresponds to the crystallographic *b*-axis. The *x*-axis is therefore perpendicular to *y*- and *z*-axes.

In this coordinate frame, which is very close to the crystal elementary cell frame [14] the Pockels tensor of $Sn_2P_2S_6$ is represented as:

$$\hat{r} = \begin{pmatrix} r_{xxx} & 0 & r_{xxz} \\ r_{yyx} & 0 & r_{yyz} \\ r_{zzx} & 0 & r_{zzz} \\ 0 & r_{yzy} & 0 \\ r_{xzx} & 0 & r_{zxz} \\ 0 & r_{yxy} & 0 \end{pmatrix}. \tag{1}$$

3. Anisotropic diffraction and self diffraction in birefringent photorefractivs

In birefringent crystals, eigenwaves with orthogonal polarizations propagate with different velocities (they have different indices of refraction). A schematic drawing of the Ewald constructions in the wavevector space for birefringent crystals is shown in Fig. 1. Suppose two waves with the wavevectors $\mathbf{k}_{1,2}$ propagate and form a fringe pattern which is imprinted inside the crystal as an index grating; it has the grating vector

$$\mathbf{K} = \mathbf{k}_1^{s,l} - \mathbf{k}_2^{s,l}. \tag{2}$$

The upper indices mark the polarizations of eigenwaves (belonging to the internal shell of Ewald construction with a smaller index of refraction n_s or external shell with a larger index n_l, respectively). For uniaxial crystals with negative birefringence like $LiNbO_3$, the smaller index *s* corresponds to extraordinary wave and larger index *l* corresponds to ordinary wave.

Recording of the index grating is most often done by the two waves that belong to the same Ewald surface (one exception is recording with spatially oscillating photovoltaic currents in $LiNbO_3$ [15]); the readout is however possible not only by one of the two recording beams (that are Bragg-matched by definition) but also with the other Bragg-matched waves. The grating vector may be translated in reciprocal space so that it touches the internal and external Ewald

#100420 - $15.00 USD Received 21 Aug 2008; revised 15 Sep 2008; accepted 15 Sep 2008; published 8 Oct 2008

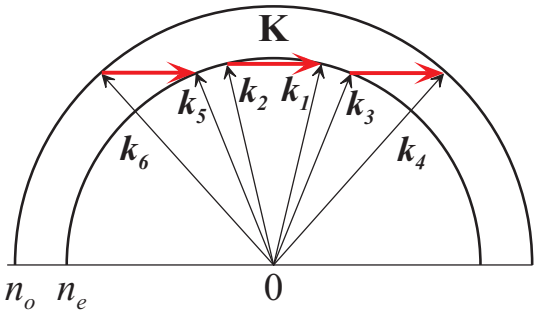

Fig. 1. Phase matching diagram for isotropic recording and anisotropic diffraction from photorefractive gratings in a birefringent crystal.

surfaces simultaneously. In this case the same grating couples two different eigenwaves of the sample that have orthogonal polarizations. The wavevectors of these waves meet one of two possible phase-matching conditions

$$\mathbf{K} = \mathbf{k}_4^{\mathrm{l}} - \mathbf{k}_3^{\mathrm{s}}, \tag{3}$$

$$\mathbf{K} = \mathbf{k}_5^{\mathrm{s}} - \mathbf{k}_6^{\mathrm{l}}. \tag{4}$$

If a wave 3 is sent to the sample at an angle defined by Eq. 3, the orthogonally polarized wave 4 appears because of the diffraction and vice versa. The same is true for waves 5 and 6, i.e., anisotropic diffraction is possible for an eigenwave with a smaller index n_s as well as for an eigenwave with larger index n_l. (For the sake of simplicity we consider all waves that propagate in the same plane defined by two recording waves, in fact the anisotropic diffraction is possible also for waves that propagate in other directions.)

The angles of readout and diffracted beams can be calculated for anisotropic diffraction from Eq. 3,4 if the refractive indices are known. The measured dependences of these angles on the recording wave angles can serve as the experimental proof of the existence of a particular anisotropic diffraction process.

For special angles of the recording beams the wavevectors of the recording and readout waves may coincide, $\mathbf{k}_3^{\mathrm{s}} = \mathbf{k}_1^{\mathrm{s}}$ or $\mathbf{k}_2^{\mathrm{s}} = \mathbf{k}_5^{\mathrm{s}}$. Thus, the diffracted waves with the orthogonal polarization appear without any auxiliary readout beams. This type of nonlinear wave mixing is called self diffraction. It is of practical interest because the selfdiffracted wave can be a phase conjugate replica of one of the recording waves providing the second wave has a plane wave front [16,17]. It is obvious that the anisotropic self diffraction can be observed only for eigenwaves with smaller index of refraction.

The phase matching conditions are a necessary prerequisite of anisotropic diffraction, but they are not sufficient for its observation. For anisotropic diffraction to occur, the crystal should possess an effective Pockels coefficient that allows two eigenwaves to be coupled. In the case of $LiNbO_3$ these coefficients are the nondiagonal components of the Pockels tensor (those with the different first two indices in the full three-index notation or r_{51} and r_{42} in contracted notation). We will show below that the expressions for the effective Pockels coefficient that couples two waves (either with identical polarizations or with orthogonal polarizations) are more complicated in low symmetry crystals like SPS.

4. Experiment

The experiment was performed with several SPS samples grown in the Institute of Solid State Physics and Chemistry, University of Uzhgorod, Ukraine. The samples are cut along the crystal-

#100420 - $15.00 USD Received 21 Aug 2008; revised 15 Sep 2008; accepted 15 Sep 2008; published 8 Oct 2008

lographic directions and typically are several mm thick. Helium Neon laser light (with TEM_{00}, 20 mW output power at 0.63 μm, linearly polarized) is used to record the photorefractive gratings. The unexpanded beams of roughly equal intensities are used to record the grating, while a third (incoherent) beam with a smaller intensity is used to readout the grating (Fig. 2). Unless otherwise stated, the recording beams impinge upon the sample symmetrically; the readout angle and the diffraction angle are measured in air from the normal to the sample input face.

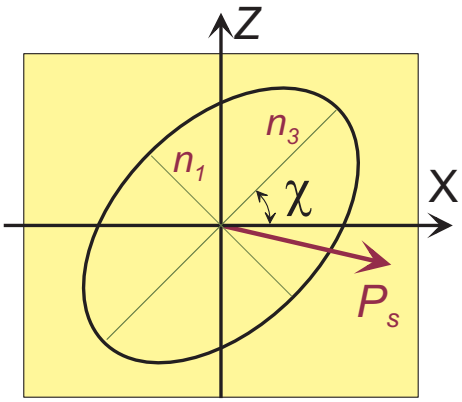

Fig. 2. Projection of the optical indicatrix of SPS crystals at ambient conditions to *xz*-plane. n_1 and n_3 are the refractive indices of eigenwaves for a *y*-cut sample.

The polarization of the recording waves is chosen to correspond to the eigenwaves polarization. In low symmetry crystals such as SPS, the optical frame does not coincide with the crystallographic frame that results in a particular orientation of eigenwaves polarization. With the *x*-cut sample, eigenwaves are polarized along *y*- or *z*-axes and for the *z*-cut sample they are polarized along *x*- or *y*-axes. For *y*-cut sample, however, the polarizations of the eigenwaves at ambient temperature are parallel neither to *x* nor to *z* directions but are tilted to $\chi = 47^\circ$ (n_1) and 43° (n_3) with respect to *x*-axis Fig.2.

In first set of experiments we concentrated on measurements of diffraction angles for anisotropic diffraction at different recording angles to identify the particular diffraction processes. Later the relative or absolute measurements of the diffraction efficiencies were performed to extract information on unknown electrooptic coefficients. The diffraction efficiencies of about 10^{-2} or higher were measured directly as a ratio of the diffracted beam intensity to the total intensity of transmitted readout and diffracted beams.

For measurement of smaller efficiencies the lock-in amplifier was used, as it is shown in Fig. 3(a), to eliminate strong scattering of the recording beams in the direction of the diffracted beam. The high-voltage amplifier (HVA) enhanced signal from the lock-in amplifier is sent to an electrooptic modulator (EOM) to modulate the readout beam with high contrast at a frequency of 1 kHz (much higher than the reciprocal decay time $\leq$ 50 1/s of a grating at the spatial frequencies used in present experiment). The signals from photodiodes PD_1 and PD_2 that measure the intensities of the diffracted and the readout beams respectively are fed into the lock-in amplifier to get the diffraction efficiency.

Anisotropic diffraction was detected in all three cuts of SPS. Fig. 4 shows the dependence of the readout and diffraction angles versus half-angle of the recording beams. The black straight lines in this figure show the trivial case of isotopic Bragg diffraction of the recording wave(s) when the diffracted wave coincides with the other recording wave. Such a diffraction was observed for recording with $\mathbf{K} \parallel x$-axis and $\mathbf{K} \parallel z$-axis; it does not occur for $\mathbf{K} \parallel y$-axis. The experimental data on isotropic diffraction are not shown in Fig. 4. The dots, squares, triangles,

#100420 - $15.00 USD Received 21 Aug 2008; revised 15 Sep 2008; accepted 15 Sep 2008; published 8 Oct 2008

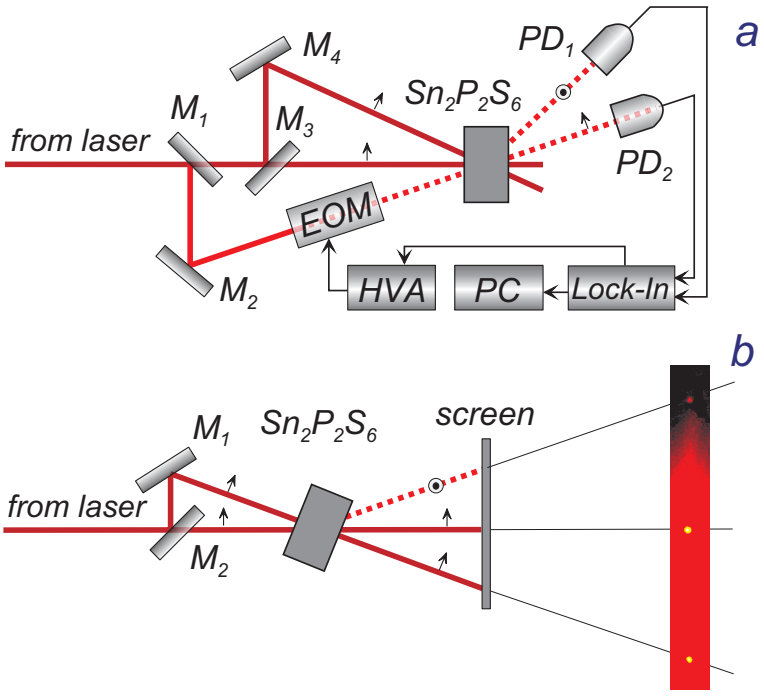

Fig. 3. Experimental arrangement to detect and study the anisotropic diffraction (a) and self diffraction (b). The intensity of the readout beam is modulated at a high frequency (1 kHz) by the electrooptic modulator EOM. The diffracted signal at the same frequency is collected from the detector PD_1 and compared with the transmitted intensity collected from the detector PD_2 by a lock-in amplifier. Only two identically polarized beams are sent to the sample to observe the self diffraction (b), for any angle between recording waves the sample tilt angle is measured for which the auxiliary beam appears with the orthogonal polarization.

and diamonds in Fig. 4 are the results for the readout and/or diffraction angles for the waves labelled 3,4,5,6 in Fig. 1 and Eqs. (3,4). The red and blue lines represent the dependences calculated from Eq. (3) and Eq. (4), respectively, with the birefringence data of SPS tabulated in [10]. A satisfactory agreement of experimental and calculated data is evident. It should be noted that the angular dependences for anisotropic diffraction shown in Fig. 4 are measured and calculated for the eigenwaves of the crystal (see Fig. 2).

To observe the anisotropic self diffraction only two beams are sent to the sample. They have identical polarizations that correspond to the smaller of the two eigenvalues of the refractive index. For any fixed recording angle the sample is rotated around the vertical axis until the diffracted beam with an orthogonal polarization appears. By adjusting different recording angles, the dependences of the diffracted angle and sample tilt angle on the recording angle can be measured. Fig. 5(a,b) shows, as an example, the results of the measurements for the *x*-cut sample. Two *y*-polarized recording beams impinge upon the sample in the *xy*-plane and generate a *z*-polarized selfdiffracted wave. The open squares in Fig. 5 show the measured values, while the solid lines represent the dependences calculated from Eq. 2 with the additional condition $\mathbf{k}_3^s = \mathbf{k}_1^s$. The self diffraction in case of $\mathbf{K} \parallel y$ (symmetric incidence of two recording waves or sample tilt angle equal to zero in Fig. 5) confirms the existence of nonvanishing r_{yzy} component of the Pockels tensor in SPS.

#100420 - $15.00 USD Received 21 Aug 2008; revised 15 Sep 2008; accepted 15 Sep 2008; published 8 Oct 2008

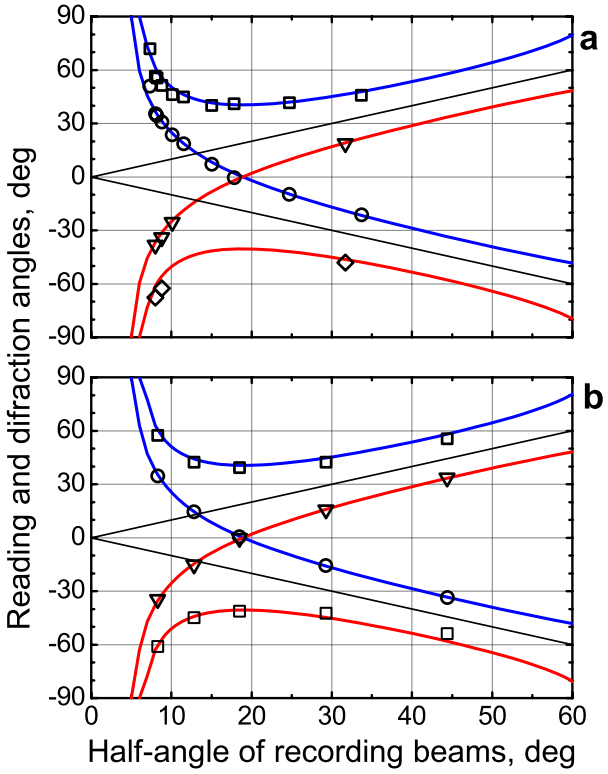

Fig. 4. Readout and diffraction angles versus recording beam angle for recording beams aligned: (a) in the *xy*-plane of the *y*-cut sample with **K** $\parallel$ *x*-axis and (b) in the *zy*-plane of the *z*-cut sample with **K** $\parallel$ *z*-axis. The solid lines represent the calculated dependences and dots, squares, triangles, and diamonds are the results of measurements, as explained in the text.

Self diffraction was observed also for the *z*-cut sample with *y*-polarized waves and for the *y*-cut sample. In the latter case, two eigenwaves with the smaller index of refraction (n_1) record the grating; its grating vector **K** can be aligned along *x*-direction as well as along *z*-direction. For all mentioned variations of self diffraction, the measured angular dependences (as shown in Fig. 5) are in good agreement with the calculated data.

It should be mentioned that self diffraction is a close relative of the light induced conical scattering that we reported recently for SPS in [18]. In conical scattering only one beam with the appropriate polarization is sent to the sample while the light scattered from the optical imperfections of the sample serves as a signal wave [8]. A cone of scattered light with the orthogonal polarization appears and its apex angle can be found from the phase matching condition of Eq. 2 providing $\mathbf{k}_3^e = \mathbf{k}_1^e$.

5. Estimating the electrooptic coefficients

Specific components of the Pockels tensor (Eq. 1) can be estimated from any nonlinear wave coupling experiment. In this study we limit ourselves to measurements of the diffraction efficiency of the recorded grating.

Within the small coupling approximation, the diffraction efficiency η of the index grating in photorefractive crystal is given by the following expression [9,19]

#100420 - $15.00 USD Received 21 Aug 2008; revised 15 Sep 2008; accepted 15 Sep 2008; published 8 Oct 2008

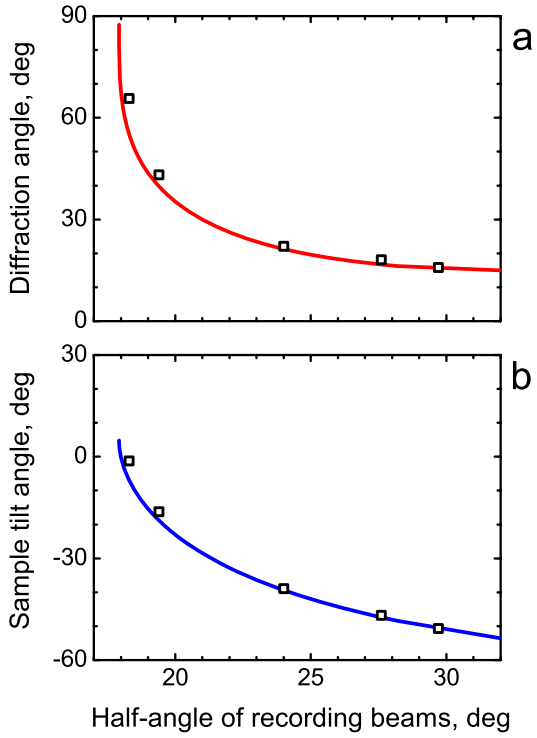

Fig. 5. Dependences of self diffraction angle (a) and sample tilt angle around the *z*-axis (b) on recording half-angle for an *x*-cut SPS crystal. Two recording waves impinge upon the sample in *xy*-plane.

$$\eta \approx \left(\frac{\pi^2 d}{\lambda^2\sqrt{k_{iz}k_{dz}}}\right)^2 \left(\vec{e}_i \cdot \delta\hat{\varepsilon} \cdot \vec{e}_d\right)^2, \tag{5}$$

with the polarization unit vectors of the diffracted and incident waves $\vec{e}_d$ and $\vec{e}_i$, respectively; longitudinal components of the wave vectors k_{iz} and k_{dz}; perturbation of the high frequency permittivity tensor $\delta\hat{\varepsilon}$; interaction length d, and light wavelength λ. From the general relationship between the perturbed tensor of high frequency dielectric impermittivity and the static electric field E, the amplitude of perturbation of the high frequency dielectric permittivity $\delta\,\hat{\varepsilon}$ can be expressed as

$$\delta\hat{\varepsilon} \approx -\hat{\varepsilon}\left(\hat{r}\vec{E}\right)\hat{\varepsilon}, \tag{6}$$

where $\hat{\varepsilon}$ is the unperturbed tensor of the high frequency dielectric permittivity. The space charge field that affects $\delta\varepsilon$ is

$$E_{sc} = K\left(\frac{k_B T}{e}\right)\frac{1}{1+K^2\ell_s^2}, \tag{7}$$

with the Boltzman constant k_B, electron charge e, spatial frequency of the grating K, and Debye screening length $\ell_s = \sqrt{\varepsilon\varepsilon_0 k_B T/e^2 N_{eff}}$. The space charge field might be much smaller than the diffusion field $K(k_B T/e)$ in case of insufficient effective trap density N_{eff} when the product of the spatial frequency and the screening length, $K^2\ell_s^2$, becomes much larger than unity.

Our aim is to extract the data on Pockels tensor components r_{ijk} from the experimentally measured values of the diffraction efficiency. As it follows from Eqs. 5-7 the efficiency depends,

#100420 - $15.00 USD Received 21 Aug 2008; revised 15 Sep 2008; accepted 15 Sep 2008; published 8 Oct 2008

apart from the effective electrooptic coefficient, on other inherent properties of the material and on the experimental conditions (wavelength, sample orientation that affects low frequency permittivity ε [20], angles of diffraction that define grating frequency K, interaction length that depends on orientation and angles). The parameters like the effective interaction length are individual characteristic of a particular sample and depend on the amount of domains with the opposite orientation of spontaneous polarization.

In order to avoid the influence of all these factors that can reduce the reliability of our estimates it is desirable to evaluate the ratios of the effective electrooptic constants when comparing, e.g., the efficiencies of isotropic and anisotropic diffraction from the same space charge grating. This was done to evaluate such components, for example, as r_{xzx} and r_{zxz}.

From Eqs. 5 and 6 we get

$$\sqrt{\frac{\eta^{(1)}}{\eta^{(2)}}} = \left| \frac{\vec{e}_d^{(1)} \hat{\varepsilon} \left(\hat{r} \vec{e}_E \right) \hat{\varepsilon} \vec{e}_i^{(1)} / \sqrt{n_d^{(1)} n_i^{(1)}}}{\vec{e}_d^{(2)} \hat{\varepsilon} \left(\hat{r} \vec{e}_E \right) \hat{\varepsilon} \vec{e}_i^{(2)} / \sqrt{n_d^{(2)} n_i^{(2)}}} \right|. \tag{8}$$

Here $\vec{e}_E$ is the static electric field unit vector, the indices (1) and (2) mark any two of several possible diffraction processes, either isotropic or anisotropic.

In general case, a certain combination of Pockels tensor components enters both in numerator and in denominator of Eq. 8. To reduce the number of components involved it is necessary to choose a particular orientation of sample and recording beams.

Let at first consider the space charge grating recorded in the y-cut sample with the grating vector **K** parallel to the x-axis. In this case, the expressions for the diffraction efficiency that enter a numerator and a denominator of Eq. 8 read

$$\sqrt{\eta_{iso1}} = C n_1^3 |r_{xxx} + r_{zzx} - (r_{xxx} - r_{zzx}) \cos 2\chi - 2 r_{xzx} \sin 2\chi|, \tag{9}$$

$$\sqrt{\eta_{iso3}} = C n_3^3 |r_{xxx} + r_{zzx} + (r_{xxx} - r_{zzx}) \cos 2\chi + 2 r_{xzx} \sin 2\chi|, \tag{10}$$

$$\sqrt{\eta_{aniso}} = C \sqrt{n_1^3 n_3^3} |(r_{xxx} - r_{zxx}) \sin 2\chi - 2 r_{xzx} \cos 2\chi|. \tag{11}$$

Here χ is the optical indicatrix rotation angle (see Fig. 2) the subscripts *iso*1 and *iso*3 mark the isotropic diffraction of the eigenwaves with indices n_1 and n_3, respectively, while *aniso* denotes the anisotropic diffraction (either of a wave with n_1 into a wave with n_3 or in the opposite direction). Finally C incorporates all mentioned above parameters that characterize the grating and experimental conditions and are identical for all possible types of diffraction from this grating.The difference in propagation directions for isotropic and anisotropic diffraction inside the sample is neglected here because a relevant correction factor appears to be less than 2 percent.

The particular weights of Pockels tensor components in any of the three equations (9-11) depend on optical indicatrix rotation angle χ. With $\chi \approx 45^\circ$ (which is very close to real value $\chi = 43^\circ$ in SPS at $\lambda = 0.63\ \mu$m and ambient conditions) equations Eqs. 9-11 are reduced to

$$\sqrt{\eta_{isox1}} \simeq C n_1^3 |r_{xxx} + r_{zzx} - 2 r_{xzx}|, \tag{12}$$

$$\sqrt{\eta_{iso3}} \simeq C n_3^3 |r_{xxx} + r_{zzx} + 2 r_{xzx}|, \tag{13}$$

$$\sqrt{\eta_{aniso}} \simeq C \sqrt{n_1^3 n_3^3} |r_{xxx} - r_{zzx}|. \tag{14}$$

From Eq. 14 it becomes clear that the anisotropic diffraction in y-cut SPS is independent of nondiagonal components r_{xzx} of the Pockels tensor while these components may affect, when being sufficiently large, the conventional isotropic diffraction. Note that this situation is quite

#100420 - $15.00 USD Received 21 Aug 2008; revised 15 Sep 2008; accepted 15 Sep 2008; published 8 Oct 2008

different from that for photorefractive crystals that belong to higher symmetry classes 4*mm* ($BaTiO_3$) or 3*m* ($LiNbO_3$), where $\chi = 0$ and where the anisotropic diffraction depends primarily on nondiagonal components of Pockels tensor.

If the data on η_{iso1}, η_{iso3}, and η_{aniso} are known from the experiment and n_1 and n_3 are known from the literature [10] one can solve the equations Eq. 12-14 for the ratios r_{zzx}/r_{xxx} and r_{xzx}/r_{xxx}. To make unambiguous conclusions about the signs of the particular components the information concerning positive direction of crystal *x*- and *z*-axes is necessary. The extracted data are given in Table 1 together with already known data from [7].

Table 1. Comparison of experimentally estimated ratios of Pockels coefficients with those known from Ref.7. In second column the values in numerator and denominator are given in pm/V units.

	previous data [7]	present paper
r_{zzx}/r_{xxx}	(140±18)/(174±10)	0.87±0.02
r_{xzx}/r_{xxx}	(-25±15)/(174±10)	-0.12±0.07

A reasonable agreement of these data proves the validity of the proposed technique and allows for evaluation of other, previously unknown, Pockels tensor components. If in the same *y*-cut sample the grating vector **K** is aligned parallel to the *z* axis the efficiencies of the three diffraction processes similar to that described by Eqs.12-14 are

$$\sqrt{\eta_{iso1}} \simeq C' n_1^3 |r_{xxz} + r_{zzz} - 2r_{zxz}|, \tag{15}$$

$$\sqrt{\eta_{isoz3}} \simeq C' n_3^3 |r_{xxz} + r_{zzz} + 2r_{zxz}|, \tag{16}$$

$$\sqrt{\eta_{aniso}} \simeq C' \sqrt{n_1^3 n_3^3} |r_{xxz} - r_{zzz}|. \tag{17}$$

With this set of equations and the measured efficiencies we can evaluate the ratios r_{xxz}/r_{zzz} and r_{zxz}/r_{zzz} that are tabulated in Table 2.

Unfortunately, the described procedure cannot be applied for all crystal cuts: for a grating vector $\mathbf{K}||y$-axis the isotropic diffraction is not allowed and there is no reference diffraction to compare with the anisotropic diffraction which is due to r_{yzy} and r_{yxy}. To follow the same procedure and evaluate the ratio of Pockels tensor components instead of absolute values, we study the anisotropic self diffraction in *x*-cut and *z*-cut samples with the grating vector **K** tilted to 45° with respect to the *y*-axis. In such a manner we get a desirable reference because the isotropic diffraction becomes possible with nonzero r_{yyz} and r_{zzz} for the *x*-cut sample (or r_{xxx} and r_{yyx} for the *z*-cut sample). Thus the anisotropic diffraction which is due to r_{yzy} (or due to r_{yxy}) can be compared to isotropic diffraction from the same grating.

For the *x*-cut sample, the efficiencies are given by

$$\sqrt{\eta_{iso1}} \simeq C'' \frac{1}{\sqrt{2}} n_2^3 |r_{yyz}|, \tag{18}$$

$$\sqrt{\eta_{iso2}} \simeq C'' \frac{1}{\sqrt{2}} \frac{n_p^5}{n_1 n_3} |r_{zzz}|, \tag{19}$$

$$\sqrt{\eta_{aniso}} \simeq C'' \sqrt{\frac{n_2^3 n_p^5}{2 n_1 n_3}} |r_{yzy}|. \tag{20}$$

with $n_p = \sqrt{(n_1^2 + n_3^2)/2}$.

#100420 - $15.00 USD Received 21 Aug 2008; revised 15 Sep 2008; accepted 15 Sep 2008; published 8 Oct 2008

A similar set of equations is derived for diffraction in the *z*-cut sample from the grating with the grating vector aligned along the bissector of *yx* angle:

$$\sqrt{\eta_{iso1}} \simeq C^* \frac{1}{\sqrt{2}} n_2^3 |r_{yyx}|, \tag{21}$$

$$\sqrt{\eta_{iso2}} \simeq C^* \frac{1}{\sqrt{2}} \frac{n_p^5}{n_1 n_3} |r_{xxx}|, \tag{22}$$

$$\sqrt{\eta_{aniso}} \simeq C^* \sqrt{\frac{n_2^3 n_p^5}{2 n_1 n_3}} |r_{yxy}|. \tag{23}$$

With the measured values of the diffraction efficiencies the equations (18-23) allow for the evaluation of the ratios r_{yyz}/r_{zzz}, r_{yzy}/r_{yyz}, r_{yyx}/r_{xxx}, and r_{yxy}/r_{yyx}. They are all given in Table 2.

Table 2. Experimentally estimated ratios of unknown Pockels coefficients.

r_{xxz}/r_{zzz}	1.7 ± 0.6
r_{yyz}/r_{zzz}	0.69 ± 0.03
r_{zxz}/r_{zzz}	-1.8 ± 0.4
$\lvert r_{yzy}/r_{yyz} \rvert$	0.06 ± 0.01
r_{zzx}/r_{xxx}	0.87 ± 0.02
r_{yyx}/r_{xxx}	0.53 ± 0.02
r_{xzx}/r_{xxx}	-0.12 ± 0.07
$\lvert r_{yxy}/r_{yyx} \rvert$	0.06 ± 0.01

The samples used in the present experiment were cut along the crystallographic axis with a precision of not better than 3°. Errors from an imperfect crystal orientation, from the approximation of the optical indicatrix orientation (45°-tilt instead of 43°-tilt with respect to *x*-axis) and from experimental errors of the diffraction efficiency measurements define the error bars shown in Table 1 and Table 2. The statistical spread of the measured data (two samples with different areas in each, reproducibility of data) was never beyond the indicated error bars.

It is worthwhile to note a quite obvious difference in the relative errors for different lines in Table 2. The general tendency is that the uncertainity is larger for the weaker components than for the stronger components. A particular relative error depends, however, on the technique of evaluation; it may appear to be larger for some components for which the set of linear equations (Eqs. 12-14 or Eqs. 15-17) should be solved to extract the data for *y*-cut sample.

As one can see, some of the Pockels coefficients can be normalized to r_{xxx} (r_{yyx} can be reduced to r_{xxx} because their ratio is known) while the others can be normalized to r_{zzz} (in similar way r_{yyz} can be reduced to r_{zzz}). To get the hierarchy of all 10 Pockels coefficients we need to normalize all components to a common coefficient, e.g., to the largest coefficient r_{xxx}. To do this it is necessary to interrelate at least two coefficients that have a different last index, one with *x* and the other with *z*. By comparing the absolute values of the diffraction efficiency for two different crystal cuts, for example, for *x*-cut and *z*-cut while keeping the polarization of the recording waves along *y* direction, the ratio r_{yyx}/r_{yyz} can be found. According to the data reported in [20] and measurements made in this study with two more SPS samples we obtain $r_{yyx}/r_{yyz} \approx 7.0 \pm 1.0$. The reliability of the last procedure is however not very high because of all of the factors discussed above (difference in domain structure seen by the recording fringes, difference in screening effects because of the anisotropy of the dielectric permittivity, etc.) Larger statistics of different SPS samples are necessary to get reliable data on the absolute values of the Pockels tensor components.

#100420 - $15.00 USD Received 21 Aug 2008; revised 15 Sep 2008; accepted 15 Sep 2008; published 8 Oct 2008

6. Conclusions

We observed and studied isotropic and anisotropic diffraction in SPS for different mutual orientations of the recording beams and sample and different polarization of the readout beam. We can summarize the main results of this study:

(i) All components of the Pockels tensor with identical first two indices (diagonal components), r_{xxx}, r_{yyx}, r_{zzx}, r_{xxz}, r_{yyz}, and r_{zzz} manifest themselves in polarization isotropic diffraction from the space charge gratings. The ratios of these components have been found via recording and reading out of photorefractive gratings in *x*-cut and *z*-cut samples.

(ii) Anisotropic diffraction in *y*-cut samples depends solely on the linear combination of the diagonal components as, for example, $r_{xxx} - r_{zzx}$. This allows for an independent check of the measured ratios of the Pockels components.

(iii) The nondiagonal components r_{xzx} and r_{zxz} are involved in isotropic diffraction in *y*-cut samples together with at least two diagonal components. To decouple a nondiagonal component it is necessary to perform three measurements of the diffraction efficiency, for isotropic diffraction of waves with two orthogonal eigenpolarizations and for anisotropic diffraction. Another possibility consists in using of data on diagonal components already available from other experiments.

(iv) Finally, the two remaining nondiagonal components of the Pockels tensor r_{yzy} and r_{yxy} are extracted from measurements of anisotropic diffraction in *x*-cut and *z*-cut samples.

Acknowledgments

The authors are grateful to Alexander Grabar and Ivan Stoyka for the SPS samples used in the present experiment. The financial support of European Office of Research and Development and Science and Technology Center of Ukraine via grant P335 is gratefully acknowledged.

#100420 - $15.00 USD Received 21 Aug 2008; revised 15 Sep 2008; accepted 15 Sep 2008; published 8 Oct 2008